COMPOSITE SCHEMES FOR CONSERVATION LAWS*

RICHARD LISKA† AND BURTON WENDROFF‡

Dedicated to the Memory of Ami Harten[1]

Abstract. Global composition of several time steps of the two-step Lax-Wendroff scheme followed by a Lax-Friedrichs step seems to enhance the best features of both, although only first order accurate. We show this by means of some examples of one-dimensional shallow water flow over an obstacle. In two dimensions we present a new version of Lax-Friedrichs and an associated second order predictor-corrector method. Composition of these schemes is shown to be effective and efficient for some two-dimensional Riemann problems and for Noh's infinite strength cylindrical shock problem. We also show comparable results for composition of the predictor-corrector scheme with a modified second order accurate WENO scheme. That composition is second order but is more efficient and has better symmetry properties than WENO alone. For scalar advection in two dimensions the optimal stability of the new predictor-corrector scheme is shown using computer algebra. We also show that the generalization of this scheme to three dimensions is unstable, but using sampling we are able to show that the composites are sub-optimally stable.

Key words. composite schemes, conservation laws, hyperbolic systems, Lax-Wendroff scheme, Lax-Friedrichs scheme, 2D Riemann problem

AMS subject classifications. 35L65, 65M06, 65M12

1. Introduction.

An evolutionary tree showing the development of finite difference methods for hyperbolic systems might emerge from the "soup" of Courant-Friedrichs-Levy and von Neumann in the form of two branches rooted in Lax-Friedrichs and Godunov. We wish to distinguish these two methods even though in one space dimension they both can be looked at as the same thing but on a different mesh arrangement, as is well-known. Godunov's idea was to start with cell averages of the initial data, and then solve the Riemann problem at each cell endpoint. For small enough time step the waves from one endpoint cannot reach a neighboring endpoint, so that the Riemann problem solutions provide the fluxes at the endpoints, and the conservation law then gives the new cell averages directly. This is a first order method in the sense of truncation error. The Godunov branch now leads us to the second order scheme of van Leer and his crucial introduction of limiters, to Ami Harten's inspired notion of total variation diminishing methods (TVD), to Roe's approximate Riemann solver, and to the current interest in essentially non-oscillatory (ENO) and weighted ENO (WENO) schemes. These methods have typically been first developed for scalar equations, then applied to systems using a field-by-field decomposition. Indeed, it seems to us that a common, even defining, feature of the Godunov descendents is the

* This work was supported in part by the CHAMMP Program of the US Department of Energy.

† Faculty of Nuclear Sciences and Physical Engineering, Czech Technical University in Prague, Břehová 7, 115 19 Prague 1, Czech Republic, (`liska@siduri.fjfi.cvut.cz`, `http://www-troja.fjfi.cvut.cz/~liska`), supported in part by the National Science Foundation International Programs grant INT-9212433, Czech Ministry of Education grant Kontakt ES 016 (1996)

‡ Group T-7, Los Alamos National Laboratory, Los Alamos, NM 87544, USA, (`bbw@lanl.gov`, `http://math.unm.edu/~bbw`)

[1]Memories: I (bw) happened to be in Tel-Aviv in June 1992 on the last day of a workshop on applied mathematics at Tel-Aviv University. I went to hear a talk by Peter Lax, and at the end of the session a group photograph was taken of the participants. As I wasn't one of them, I was lurking off to one side. Ami grabbed me and placed me next to Peter in the front row, saying that there weren't that many opportunities to get a picture of Lax and Wendroff together. I was very moved but not surprised by this example of Ami's warm and generous nature.

need for an expansion in the eigenvectors of the gradient of the flux function. The positive schemes of [12] also use an eigenvector expansion. The ENO method also treats space and time independently; it is basically a method of lines, solving the system of ordinary differential equations by a Runge-Kutta technique. These methods achieve very high quality solutions, but they are costly both because of the local eigenvector expansions and the Runge-Kutta steps.

For the system

$$U_t = f_x(U)$$

Lax-Friedrichs defines new values on a staggered dual grid as

$$U_{i+1/2}^{n+1/2} = \frac{1}{2}[U_i^n + U_{i+1}^n] + \frac{\Delta t}{2\Delta x}[f(U_{i+1}^n) - f(U_i^n)], \tag{1.1}$$

with standard notation. Then the solution on the primary grid is obtained by repeating the above step with the indices shifted by 1/2. This is simplicity itself, robust, but inaccurate because it is formally first order accurate and excessively diffusive. The evolutionary path from Lax-Friedrichs leads to Lax-Wendroff, which in its two-step form simply uses the first half step of Lax-Friedrichs as a predictor to get the fluxes centered in time, that is,

$$U_i^{n+1} = U_i^n + \frac{\Delta t}{\Delta x}[f(U_{i+1/2}^{n+1/2}) - f(U_{i-1/2}^{n+1/2})]. \tag{1.2}$$

This too has the virtue of simplicity and it is formally second order accurate, but unless the data is smooth it suffers from excessive oscillations.

There has been the analogue of a biological explosion of methods designed to correct the deficiencies of these simple schemes. Anti-diffusion was proposed in [1] to improve the resolving power of Lax-Friedrichs, but although anti-diffusion does very well with shock type discontinuities it introduces severe staircase distortions in smooth regions. Following von Neumann, Lax and Wendroff [18] proposed artificial viscosity as a way to reduce oscillations in their method, and many variants of this idea can be found. Finding a good artificial viscosity still seems to be more of an art than a science, but this remains a reasonable approach. The self-adjusting hybrid schemes of Harten and Zwas [7] switch from a diffusive scheme like Lax-Friedrichs in the neighborhood of a discontinuity to a second order method like Lax-Wendroff elsewhere. Designing the switch is as much of an art as is designing an artificial viscosity. Another possibility is the use of a variation diminishing filter as proposed by Engquist et al [6]. However, that filter seems to work best when used with a field-by-field decomposition; in our experience with the shallow water equations the filter applied to the conserved variables caused unacceptable errors in the smooth parts of the flow. The Godunov idea without eigenvector decomposition through the use of a simple approximate Riemann solver has been implemented in [5].

We propose here to remain in the Lax-Friedrichs species by using a global composition of schemes. It occurred to us that perhaps one should use a filter that is consistent with the differential equations; for example, use Lax-Friedrichs as a filter for Lax-Wendroff. This leads to the following. Let L_W be the two-step operator in (1.2) mapping grid data at time n to the data at time $n+1$, and let L_F be the corresponding operator defined by (1.1). Then let S_k be the difference operator defined by doing $k-1$ applications of L_W followed by one application of L_F.

$$S_k = L_F \circ L_W \circ \cdots \circ L_W,$$

so that

$$U^{n+k} = S_k U^n.$$

We will call such a composite scheme the LWLFk scheme.

This is not a new idea, as Len Margolin has pointed out, since some meteorological codes compose the oscillatory second order leap-frog scheme with diffusive backward Euler in this way. We are going to show by means of several examples that this Lax-Wendroff Lax-Friedrichs composition works remarkably well. We will first present some computations of one-dimensional shallow water flow over an obstacle. We then derive a new two-dimensional Lax-Friedrichs and an associated two-step second order accurate optimally stable scheme. We compute some two-dimensional Riemann problems using composition of these methods. This composite idea also seems to well-preserve cylindrical symmetry and accuracy in Noh's classical infinite strength cylindrical shock problem. Although these composites have good resolving power for shocks, they are only first order accurate. Second order accuracy can be achieved by composing the predictor-corrector with a second order diffusive scheme. One such is second order WENO applied to the conserved variables rather than to the characteristic variables. We do some of the same examples with this method. This works very well on the shallow water problem and on Noh's problem, but not as well on the two-dimensional Riemann problems Finally, using computer algebra we analyze the stability of the new predictor-corrector scheme for the scalar advection equation in two or three dimensions. Unfortunately, it is unstable in three dimensions, however, the associated schemes composed with Lax-Friedrichs are sub-optimally stable.

2. Shallow water flow over an obstacle. As is well-known the Lax-Friedrichs (LF) scheme is too diffusive and smears out the shocks. On the other hand the Lax-Wendroff (LW) scheme without artificial viscosity resolves steep shocks but it is highly oscillatory close to the shocks. The problem of shallow water flow over topography illustrates this dramatically, indeed, it was this problem that led us to consider composite schemes in [15].

For modeling of a shallow water flow over topography in 1D the shallow water equations [10]

$$\begin{aligned} h_t + (hu)_x &= 0 \\ (hu)_t + \left(hu^2 + g\frac{1}{2}h^2\right)_x + ghz_{0x} &= 0. \end{aligned}$$

are used. Here $h(x,t)$ is the thickness of the water layer, $u(x,t)$ is the velocity of the layer, $z_0(x)$ is the height of the bottom profile and g is the gravitational constant.

For the examples presented here we take $g = 1$ and we solve the initial-boundary value problem on the space interval $x \in (A_x, B_x), A_x < 0, B_x > 0$ with initial conditions

$$h(x,0) + z_0(x) = 1, \quad u(x,0) = u_0,$$

free boundary conditions

$$h_x(A_x,t) = 0, \quad u_x(A_x,t) = 0, \quad h_x(B_x,t) = 0, \quad u_x(B_x,t) = 0,$$

and the bottom profile from [10]

$$z_0(x) = \begin{cases} b_c\left(1 - \frac{x^2}{4}\right) & \text{for } -2 \le x \le 2 \\ 0 & \text{otherwise.} \end{cases}$$

For the first example here we use $b_c = 0.2$, $u_0 = 1$ and solve it in $x \in (-10, 10)$. The results of standard Lax-Friedrichs and Lax-Wendroff schemes using 250 points are presented in Fig. 2.1, and the oscillations LW and the diffusion of LF are very evident.

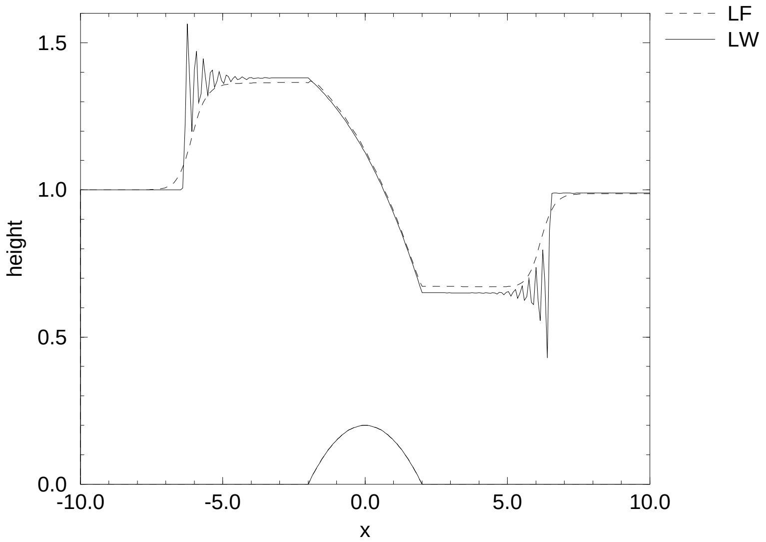

FIG. 2.1. *Comparison of heights for the shallow water problem with $b_c = 0.2, u_0 = 1$ at $t = 20$ calculated by Lax-Friedrichs and Lax-Wendroff two-step schemes using 250 points.*

The results of the same problem treated by the LWLF4 composite scheme are presented in Fig. 2.2 using 250 and 2000 points. It appears quite clear that the composite resolves the shocks better than LF but does not suffer from the oscillations of LW. An heuristic explanation of this is that on the average per time step the first order truncation error of Lax-Friedrichs is reduced by 1/4-th while the amplification factor is raised to the 1/4-th power.

There are several ways to remove oscillations from the results of the LW scheme, however, none of these is completely satisfactory. In Fig. 2.3 we present the results of the same shallow water problem calculated by LW method with the filter proposed by Engquist *et al.* [6]. The filter is applied to every component $v \in (h, hu)$ in each grid point in which v_j is a local extremum, that is when $d_j^+ d_j^- < 0$ where d_j^+, d_j^- are differences

$$d_j^+ = v_{j+1} - v_j, \quad d_j^- = v_j - v_{j-1} \tag{2.1}$$

So if $d_j^+ d_j^- < 0$ then v_j is corrected by

$$v_j = v_j + \delta_j \operatorname{sign} d_j^+$$

where

$$\delta_j = \min\left(\min(|d_j^+|, |d_j^-|), \frac{1}{2}\max(|d_j^+|, |d_j^-|)\right).$$

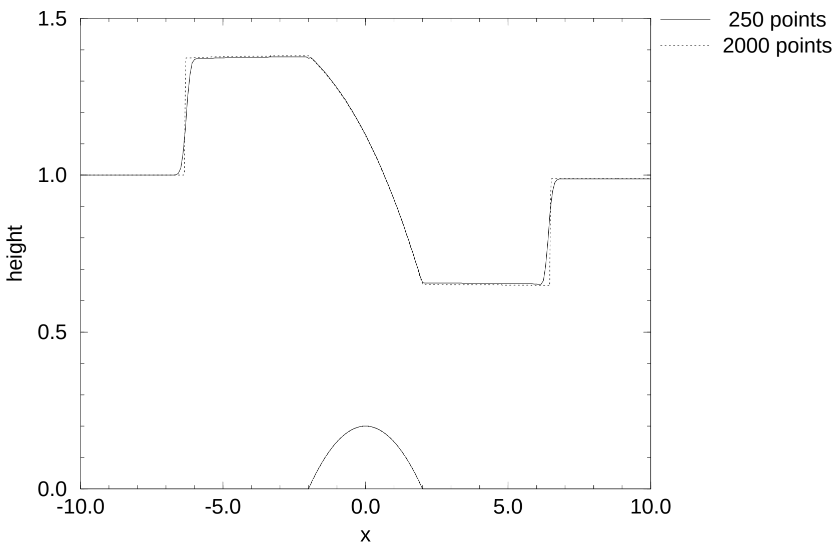

FIG. 2.2. *Comparison of heights for the shallow water problem with $b_c = 0.2, u_0 = 1$ at $t = 20$ calculated by the composite LWLF4 scheme with 250 and 2000 points.*

Further to retain conservation one of v_{j-1}, v_{j+1} must be corrected in the opposite sense according to

$$v_J = v_J - \delta_j \operatorname{sign} d_j^+$$

where $J = j + 1$ for $|d_j^+| > |d_j^-|$ and $J = j - 1$ otherwise. The filter removes the unwanted oscillations but it introduces quite bad behavior in other smooth parts of the solution. We should note here that this filter is the simplest one presented in [6].

One way to decrease the extreme diffusion of the Lax-Friedrichs scheme is to use the anti-diffusion proposed in [13]. The anti-diffusion correction which applies to all components $v \in (h, hu)$

$$v_j = v_j - \alpha_j + \alpha_{j-1}$$

is defined in terms of forward and backward differences (2.1) by

$$\alpha_j = \frac{1}{2} \max\left(0, \min(d_{j+1}^+ \operatorname{sign} d_j^+, |d_j^+|/2, d_{j-1}^+ \operatorname{sign} d_j^+)\right) \operatorname{sign} d_j^+.$$

Note that the anti-diffusion correction is applied only in regions where the component v is monotone. It serves to cancel the diffusion introduced by the averaging in LF, but it is limited so as to maintain positivity in the scalar case. However as can be seen in Fig. 2.4 it introduces a familiar staircase behavior in some smooth regions of the solution, again especially on the downstream side of the bump. In this figure we present results of the shallow water model with $b_c = 0.8, u_0 = 0.6$ at $t = 20$ done by the Lax-Friedrichs scheme with anti-diffusion (LFAD) and with the composite LWLF4 scheme. We present also the results of the LWLF4 scheme on a fine grid with 2000 points to show the "exact" solution. Note that the result of the composite LWLF4

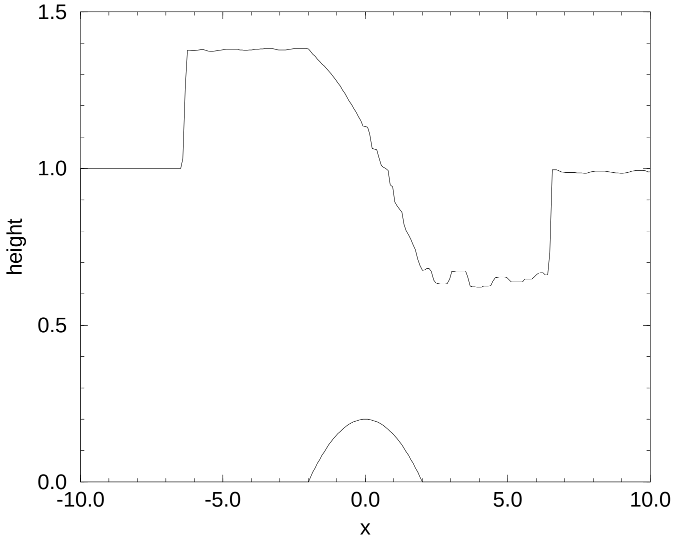

FIG. 2.3. *Heights for the shallow water problem with* $b_c = 0.2, m_0 = 1$ *at* $t = 20$ *calculated by Lax-Wendroff two-step scheme with the filter using 250 points.*

scheme on the coarse grid is also not completely free of problems as it has a dip at $x = -2$ where the profile of the bottom is not smooth.

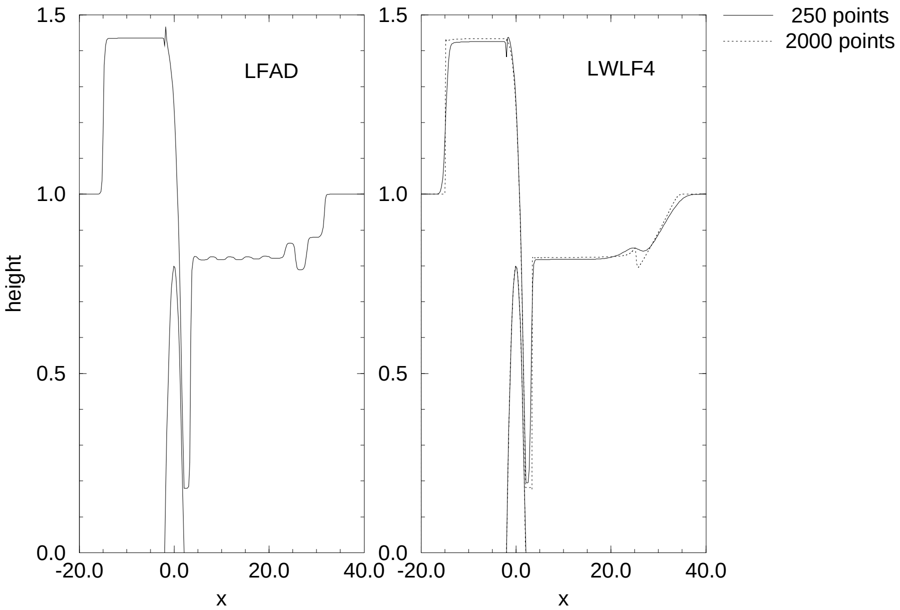

FIG. 2.4. *Comparison of heights for the shallow water problem with* $b_c = 0.8, u_0 = 0.6$ *at* $t = 20$ *calculated by the Lax-Friedrichs two-step scheme with anti-diffusion (LFAD)and the composite LWLF4 scheme using 250 points for LFAD and 250 and 2000 points for LWLF4 schemes.*

3. A two-dimensional composite scheme. There are two predictor-corrector versions of Lax-Wendroff that we know of. One is Richtmyer's [18] staggered grid version, but see also Wendroff [22] for an n-dimensional statement and stability analysis. The other is due to Eilon *et al* [4] and uses a straightforward extension of Lax-Friedrichs to two dimensions as a predictor. Neither these nor the original formulation are optimally stable. Of course, the Strang dimensional splittings are optimally stable, that is, the two-dimensional stability condition is just that the one-dimensional operators should be stable. However, we would like to maintain a multi-dimensional flavor here, so we will not consider dimensional splitting, but instead we offer an apparently new version of Lax-Friedrichs and the associated predictor-corrector scheme that is provably optimally stable for the scalar advection equation. Our experiments with two-dimensional gas dynamics appear to show optimal stability for that system as well. The scheme is based on the observation of Boukadida and LeRoux [2] that in order to implement a two-dimensional Godunov method to get cell averages on the dual grid from the averages on the primary grid one need only solve one-dimensional Riemann problems on the edges of the dual grid, see Fig. 3.1, provided that the time step is sufficiently small that the disturbance produced at the center of the cell does not reach the edges. More precisely, for the system

$$U_t = f_x(U) + g_y(U)$$

we have

$$\begin{aligned} U^{n+1/2}_{i+1/2,j+1/2} &= \frac{1}{4}[U^n_{i,j} + U^n_{i+1,j} + U^n_{i,j+1} + U^n_{i+1,j+1}] \\ &+ \frac{\Delta t}{2\Delta x}[F_{i+1,j+1/2} - F_{i,j+1/2}] + \frac{\Delta t}{2\Delta y}[G_{i+1/2,j+1} - G_{i+1/2,j}], \end{aligned} \tag{3.1}$$

where

$$F_{i+1,j+1/2} = \frac{1}{\Delta t \Delta y}\int_{y_j}^{y_{j+1}}\int_0^{\Delta t/2} f(\hat{U}(x_{i+1}, y, t))dt\, dy,$$

and $\hat{U}(x_{i+1}, y, t)$ is the solution, as a function of y and t, of the Riemann problem with initial data

$$\hat{U}(x_{i+1}, y, 0) = \begin{cases} U^n_{i+1,j} & \text{for } y < y_{j+1/2} \\ U^n_{i+1,j+1} & \text{for } y > y_{j+1/2}. \end{cases}$$

Similarly,

$$G_{i+1/2,j+1} = \frac{1}{\Delta t \Delta x}\int_{x_i}^{x_{i+1}}\int_0^{\Delta t/2} g(\hat{U}(x, y_{j+1}, t))dt\, dx,$$

and $\hat{U}(x, y_{j+1}, t)$ is the solution, as a function of x and t, of the Riemann problem with initial data

$$\hat{U}(x, y_{j+1}, 0) = \begin{cases} U^n_{i,j+1} & \text{for } x < x_{i+1/2} \\ U^n_{i+1,j+1} & \text{for } x > x_{i+1/2}. \end{cases}$$

We propose to replace the integrated exact Riemann solutions by a one-dimensional Lax-Friedrichs approximation, obtaining the fluxes

$$F_{i+1,j+1/2} = f\left(\frac{1}{2}[U_{i+1,j+1} + U_{i+1,j}] + \frac{\Delta t}{4\Delta y}[g(U_{i+1,j+1}) - g(U_{i+1,j})]\right), \tag{3.2}$$

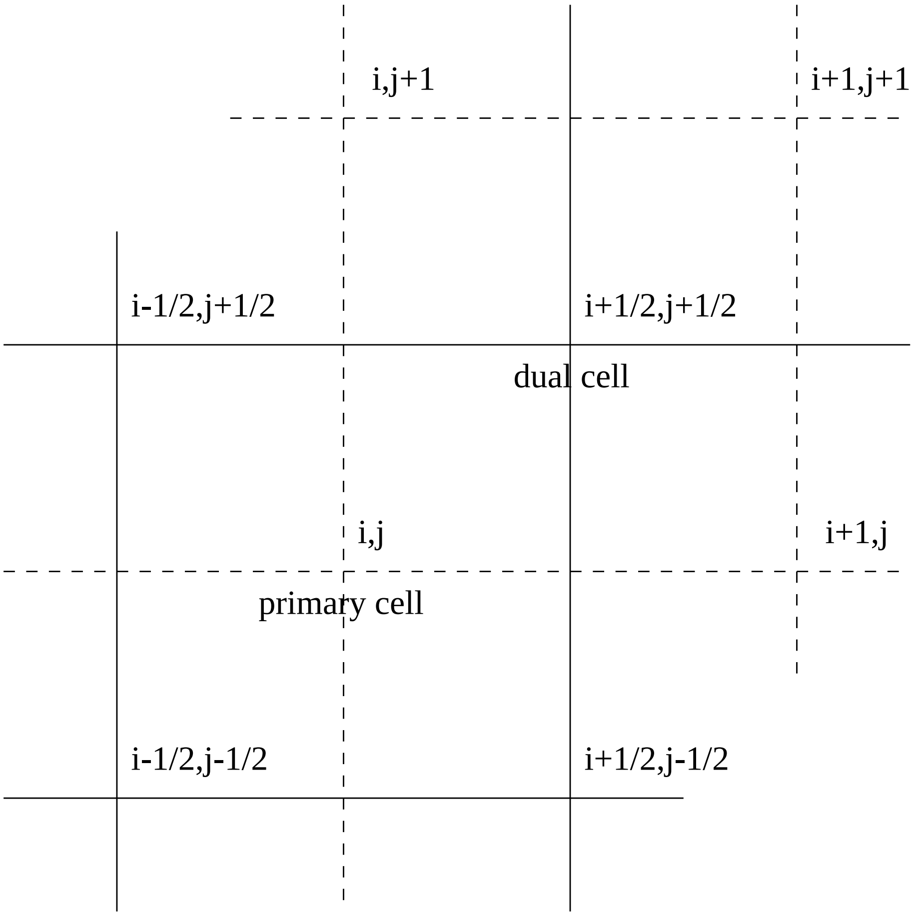

FIG. 3.1. *Staggered grid in 2D, primary grid is shown as solid lines and staggered dual grid as dashed lines*

and

$$G_{i+1/2,j+1} = g\left(\frac{1}{2}[U_{i+1,j+1} + U_{i,j+1}] + \frac{\Delta t}{4\Delta x}[f(U_{i+1,j+1}) - f(U_{i,j+1})]\right). \tag{3.3}$$

In case U is scalar and

$$f(U) = aU, \qquad g(U) = bU, \tag{3.4}$$

these fluxes agree with the fluxes obtained from the exact Riemann solver, and, as noted by Boukadida and LeRoux, the scheme then is just transport projection, that is,

$$\begin{aligned} 4U^{n+1/2}_{i+1/2,j+1/2} = {} & (1+\lambda)(1+\mu)U_{i+1,j+1} + (1+\lambda)(1-\mu)U_{i+1,j} \\ & +(1-\lambda)(1+\mu)U_{i,j+1} + (1-\lambda)(1-\mu)U_{i,j}, \end{aligned} \tag{3.5}$$

where

$$\lambda = a\Delta t/\Delta x, \qquad \mu = b\Delta t/\Delta y. \tag{3.6}$$

The second order accurate predictor-corrector scheme is then

$$
\begin{aligned}
U_{i,j}^{n+1} &= U_{i,j}^{n} \\
&+ \frac{\Delta t}{2\Delta x}[f(U_{i+1/2,j+1/2}) + f(U_{i+1/2,j-1/2}) - f(U_{i-1/2,j+1/2}) - f(U_{i-1/2,j-1/2})] \\
&+ \frac{\Delta t}{2\Delta y}[g(U_{i+1/2,j+1/2}) + g(U_{i-1/2,j+1/2}) - g(U_{i+1/2,j-1/2}) - g(U_{i-1/2,j-1/2})].
\end{aligned}
\tag{3.7}
$$

We show in §4 that for scalar advection (3.4) this is an optimally stable method, that is, the stability condition is $\max(|\lambda|, |\mu|) \leq 1$.

We call this second order method CF, for corrected Lax-Friedrichs, and the first order scheme consisting of two applications of ((3.1)) with (3.2)) and ((3.3) will be denoted by LF. The composite is

$$
LF \circ CF \circ \cdots \circ CF \tag{3.8}
$$

and is called CFLFn, consisting of $n-1$ applications of CF followed be one LF.

3.1. Three gas dynamic tests. In [19] and [12] a suite of two-dimensional Riemann problems for an ideal gas was computed. We have chosen two to do with the composite CFLF4. The initial data consists of a single constant state in each of four quadrants of the $x-y$ plane. The problem is solved in the $x-y$ region $(0,1)\times(0,1)$ and the four quadrants are given by dividing this region by two lines $x = 1/2, y = 1/2$. We will use the subscripts ll, lr, ul, ur to denote lower-left, lower-right, upper-left and upper-right quadrants respectively. These constant states are chosen so that each pair of one-dimensional Riemann problems produces a single wave, which could be a shock, rarefaction or slip contact discontinuity.

The Euler equations for an ideal gas in 2D are

$$
U_t + F(U)_x + G(U)_y = 0,
$$

where

$$
U = \begin{pmatrix} \rho \\ \rho u \\ \rho v \\ \rho E \end{pmatrix}, \quad F = \begin{pmatrix} \rho u \\ \rho u^2 + p \\ \rho u v \\ u(\rho E + p) \end{pmatrix}, \quad G = \begin{pmatrix} \rho v \\ \rho u v \\ \rho v^2 + p \\ v(\rho E + p) \end{pmatrix}.
$$

Here ρ is the density, u the velocity in the x-direction, v the velocity in the y direction, $E = e + 1/2(u^2 + v^2)$ is the total energy, e is the internal energy density, and $p = (\gamma - 1)\rho e$ is the pressure.

Our first example is configuration 4 of [12] in which each of the waves is a shock. The initial conditions for $V = (p, \rho, u, v)$ in the four quadrants are $V_{ll} = (1.1, 1.1, 0.8939, 0.8939)$, $V_{lr} = (0.35, 0.5065, 0, 0.8939)$, $V_{ul} = (0.35, 0.5065, 0.8939, 0)$, $V_{ur} = (1.1, 1.1, 0, 0)$. The grid size is 400 by 400, the time steps are variable and chosen so that

$$
\max(|u \pm c|\Delta t/\Delta x, |v \pm c|\Delta t/\Delta y) \leq 1 \tag{3.9}
$$

where u and v are the x and y components of velocity and c is the speed of sound. We also force LF on the last time step. The result of this example at $t = 0.25$ calculated by the CFLF4 method is presented in Fig. 3.2 as a contour plot of density with 30 contour level lines. The dips on the contour plot close to the curved shocks which are bigger for the upper-right curved shock than for the lower-right one are caused by an overshoot at the top of the shock.

Contour plots can sometimes be misleading, so in order to see more details of the numerical solution we present in Fig. 3.3, a surface plot of density for the representative region $(x, y) \in (0.75, 1) \times (0.25, 0.5)$, but computed on a finer 800 by 800 grid over the whole domain. For clarity we have plotted every fourth grid line in each direction.

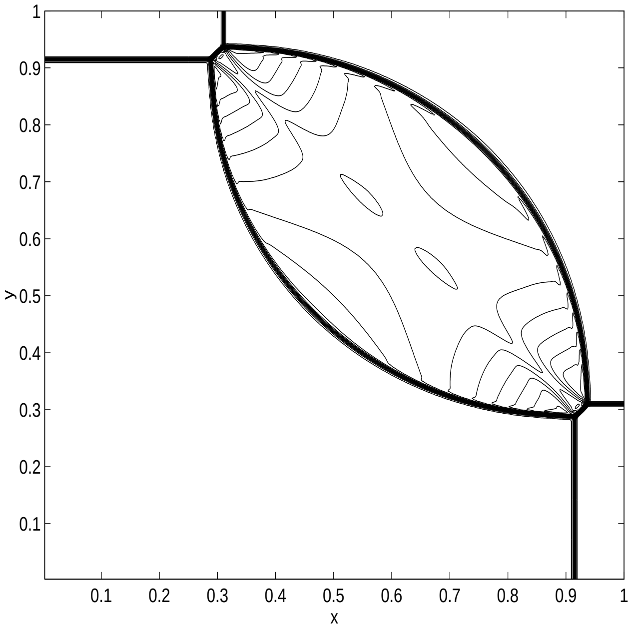

FIG. 3.2. *Contour plot of density for the 2D Riemann problem for an ideal gas with* $\gamma = 1.4$ *for configuration 4 done with the CFLF4 scheme at* $t = 0.25$*, 269 time steps,* $\Delta x = \Delta y = 1/400$*, 30 contours.*

The second example is configuration 6 of [12] in which each of the waves is a slip line. The initial conditions in the four quadrants are $V_{ll} = (1, 1, -0.75, 0.5), V_{lr} = (1, 3, -0.75, -0.5), V_{ul} = (1, 2, 0.75, 0.5), V_{ur} = (1, 1, 0.75, -0.5)$. The result of this example at $t = 0.3$ calculated by the CFLF6 method is presented in Fig. 3.4 again with 30 contour level lines. Note that we have done nothing to enhance the resolution of contact discontinuities.

The third example is a classic test of W. Noh [17] for an ideal gas with $\gamma = 5/3$. The initial density is 1, the initial pressure is 0, and the initial velocities are directed toward the origin with magnitude 1. The solution is an infinite strength circularly symmetric shock reflecting from the origin; the density behind the shock is 16 (compare with the Fig. 3.6), the shock speed is 1/3 and ahead of the shock, that is for $\sqrt{x^2 + y^2} > t/3$, the density is $(1 + t/\sqrt{x^2 + y^2})$. The computational domain is $0 \le x \le 1$, $0 \le y \le 1$. At the boundaries $x = 1$ and $y = 1$ we used the exact density as a function of time and radius together with the initial pressure and velocity. The grid size is 75 by 75. Fig. 3.5 is a contour plot of density with the CFLF4 scheme at the time $t = 1$. In Fig. 3.6 we show the variation of density along the diagonal $x = y$.

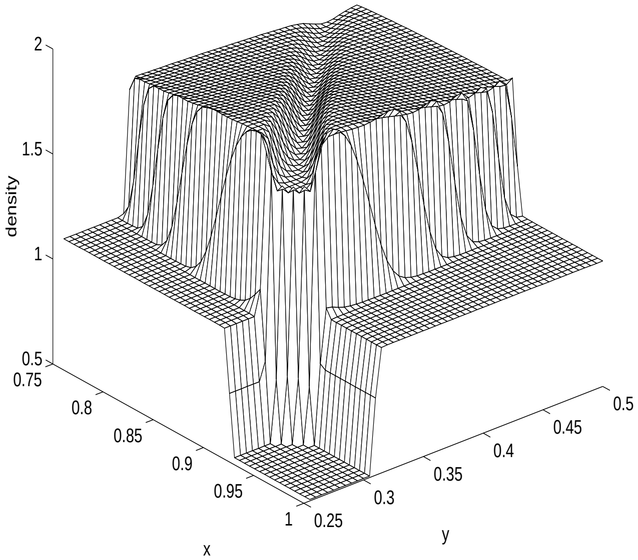

FIG. 3.3. *Surface plot of density in the region* $(x,y) \in (0.75,1) \times (0.25,0.5)$ *for the 2D Riemann problem for an ideal gas for configuration 4 with* $\gamma = 1.4$ *done with the CFLF4 scheme at* $t = 0.25$, *550 time steps,* $\Delta x = \Delta y = 1/800$

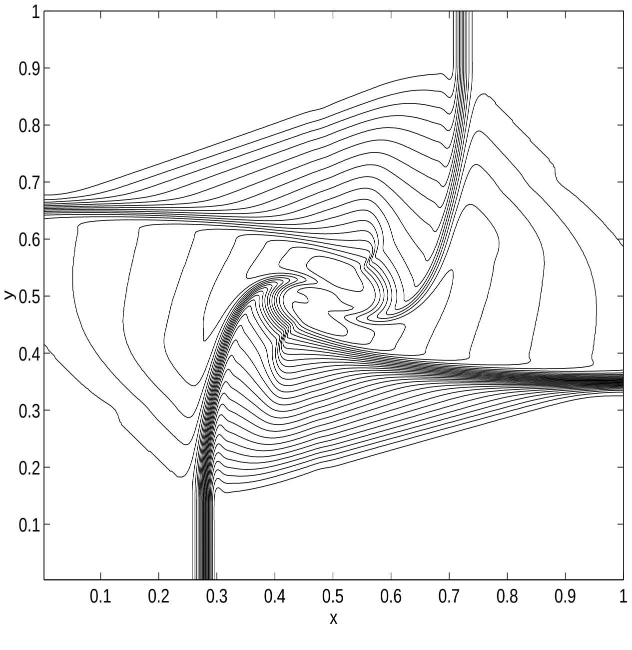

FIG. 3.4. *Contour plot of density for the 2D Riemann problem for an ideal gas with* $\gamma = 1.4$ *for configuration 6 done with the CFLF6 scheme at* $t = 0.3$, *244 time steps,* $\Delta x = \Delta y = 1/400$, *30 contours.*

This is a difficult problem. The Lagrangian codes dealing with this problem suffer from a very large error in the density at the center. We must admit to being pleasantly surprised that the composite does as well as the figure shows. The central error is quite small, and just as satisfying is the maintenance of circular symmetry.

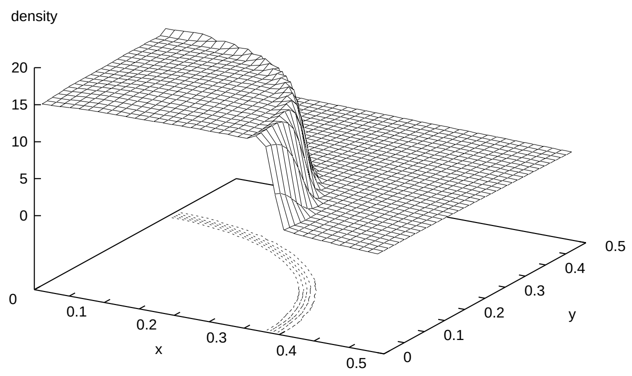

FIG. 3.5. *Surface and contour plot of density for the Noh problem at time $t = 1$ computed by CFLF4 scheme on a 75 by 75 grid.*

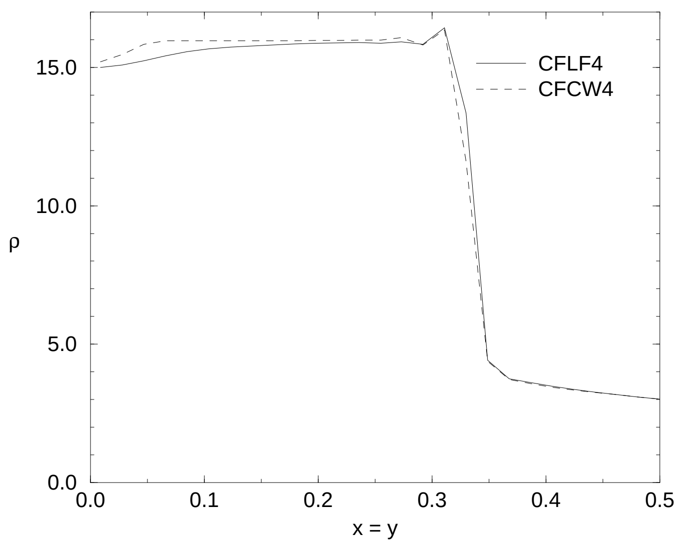

FIG. 3.6. *Density profile of the Noh problem at time $t = 1$ computed by CFLF4 scheme and CFCW4 2-nd order scheme (see §5) on 75 by 75 grid on the diagonal line $x = y$.*

4. Stability analysis for scalar advection. In this section we analyze the stability of the predictor-corrector and composite schemes used for the 2D scalar advection equation

$$u_t = au_x + bu_y \tag{4.1}$$

and for the 3D scalar advection equation

$$u_t = au_x + bu_y + cu_z. \tag{4.2}$$

We start with the analysis of the predictor scheme for the advection equation (3.5). It is a positive scheme for $\max(|\lambda|, |\mu|) \leq 1$, so it is stable and so also the two step LF scheme is stable for all such λ, μ.

The second order predictor-corrector scheme for (4.1) is given by the predictor (3.5) and the corrector (3.7), with (3.6) and (3.4). Using the computer algebra system Reduce [8] with the package FIDE [14] we have found after Fourier transformation

$$u_{i,j} = \bar{u}e^{\imath(i\alpha+j\beta)}$$

the amplification factor of this scheme is

$$|f|^2 = 1 + \frac{4\left[\tan(\alpha/2)\lambda + \tan(\beta/2)\mu\right]^2}{\left[\tan^2(\alpha/2)+1\right]^2\left[\tan^2(\beta/2)+1\right]^2} \left[\tan^2(\alpha/2)\tan^2(\beta/2)(\lambda^2\mu^2-1) + \tan^2(\alpha/2)(\lambda^2-1) + \tan^2(\beta/2)(\mu^2-1)\right]$$

As can easily be seen $|f|^2 \leq 1$ iff $|\lambda| \leq 1 \wedge |\mu| \leq 1$ so the scheme is optimally stable.

In Fig. 4.1 we present the dependence of the effective amplification factor $|f|^{1/n}$ on the angles $\alpha = \beta$ for the case $\lambda = \mu = 1/2$ and several composite CFLFn schemes. The choice $n = 4$ seems to flatten out the amplification while providing sufficient diffusion.

In 3D we can extend the ideas of the 2D predictor corrector schemes to get for the scalar advection equation (4.2) the transport projection predictor

$$\begin{aligned} 8u^{n+1/2}_{i+1/2,j+1/2,k+1/2} = \\ &(1+\lambda)(1+\mu)(1+\tau)u_{i+1,j+1,k+1} + (1+\lambda)(1+\mu)(1-\tau)u_{i+1,j+1,k} \\ &+(1+\lambda)(1-\mu)(1+\tau)u_{i+1,j,k+1} + (1+\lambda)(1-\mu)(1-\tau)u_{i+1,j,k} \\ &+(1-\lambda)(1+\mu)(1+\tau)u_{i,j+1,k+1} + (1-\lambda)(1+\mu)(1-\tau)u_{i,j+1,k} \\ &+(1-\lambda)(1-\mu)(1+\tau)u_{i,j,k+1} + (1-\lambda)(1-\mu)(1-\tau)u_{i,j,k}, \end{aligned} \tag{4.3}$$

where λ, μ are given by (3.6) and $\tau = c\Delta t/\Delta z$. If we apply the predictor again for the half step from time level $n + 1/2$ to n we obtain the two-step new Lax-Friedrichs 3D scheme. As in the case of two dimensions we can now construct the second order corrector

$$\begin{aligned} u^{n+1}_{i,j,k} = u^n_{i,j,k} + \frac{1}{4}\Big[\lambda(&u^{n+1/2}_{i+1/2,j+1/2,k+1/2} + u^{n+1/2}_{i+1/2,j+1/2,k-1/2} \\ &+u^{n+1/2}_{i+1/2,j-1/2,k+1/2} + u^{n+1/2}_{i+1/2,j-1/2,k-1/2} \\ &-u^{n+1/2}_{i-1/2,j+1/2,k+1/2} - u^{n+1/2}_{i-1/2,j+1/2,k-1/2} \\ &-u^{n+1/2}_{i-1/2,j-1/2,k+1/2} - u^{n+1/2}_{i-1/2,j-1/2,k-1/2}) \end{aligned}$$

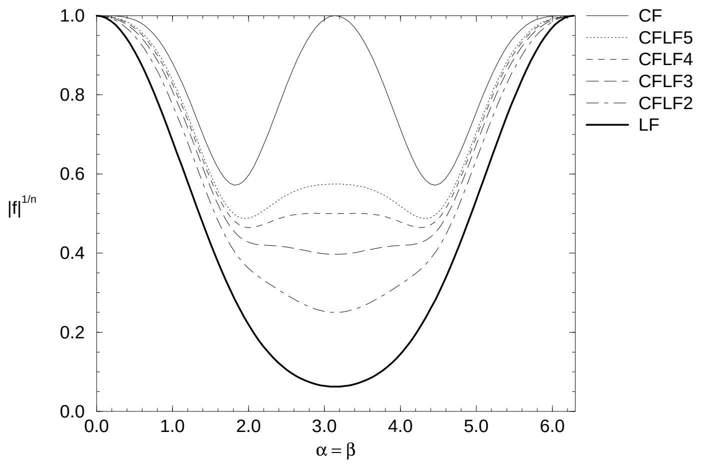

FIG. 4.1. *Dependence of the effective amplification factor per one time step on angles* $\alpha = \beta$ *for the case* $\lambda = \mu = 1/2$ *for CF,CFLF5,CFLF4,CFLF3,CFLF2,LF schemes (in the order from top to down in the figure as in the legend).*

$$
\begin{aligned}
&+\mu(u^{n+1/2}_{i+1/2,j+1/2,k+1/2} + u^{n+1/2}_{i+1/2,j+1/2,k-1/2}\\
&\quad +u^{n+1/2}_{i-1/2,j+1/2,k+1/2} + u^{n+1/2}_{i-1/2,j+1/2,k-1/2}\\
&\quad -u^{n+1/2}_{i+1/2,j-1/2,k+1/2} - u^{n+1/2}_{i+1/2,j-1/2,k-1/2}\\
&\quad -u^{n+1/2}_{i-1/2,j-1/2,k+1/2} - u^{n+1/2}_{i-1/2,j-1/2,k-1/2})\\
&+\tau(u^{n+1/2}_{i+1/2,j+1/2,k+1/2} + u^{n+1/2}_{i+1/2,j-1/2,k+1/2}\\
&\quad +u^{n+1/2}_{i-1/2,j+1/2,k+1/2} + u^{n+1/2}_{i-1/2,j-1/2,k+1/2}\\
&\quad -u^{n+1/2}_{i+1/2,j+1/2,k-1/2} - u^{n+1/2}_{i+1/2,j-1/2,k-1/2}\\
&\quad -u^{n+1/2}_{i-1/2,j+1/2,k-1/2} - u^{n+1/2}_{i-1/2,j-1/2,k-1/2})\Big] .
\end{aligned}
\tag{4.4}
$$

We have called this predictor-corrector scheme the corrected Lax-Friedrichs (CF) scheme. With the use of computer algebra we have obtained the amplification factor of this scheme as

$$|f|^2 = 1 + 4A\frac{\lambda\mu\tau\tan(\alpha/2)\tan(\beta/2)\tan(\gamma/2)D + AB}{D^2}$$

where

$$
\begin{aligned}
A &= \lambda\tan(\alpha/2) + \mu\tan(\beta/2) + \tau\tan(\gamma/2)\\
B &= \sum_{j=0}^{1}\sum_{k=0}^{1}\sum_{m=0}^{1}\tan^{2j}(\alpha/2)\tan^{2k}(\beta/2)\tan^{2m}(\gamma/2)(\lambda^{2j}\mu^{2k}\tau^{2m} - 1)\\
D &= (\tan(\alpha/2)^2 + 1)(\tan(\beta/2)^2 + 1)(\tan(\gamma/2)^2 + 1)
\end{aligned}
$$

This formula is quite complicated and hard to analyze. However we have succeeded to do the algebraic analysis for the one special case $\mu = \tau = \lambda, \gamma = \pi/2$ for which the amplification factor is

$$|f|^2 = 1 + \frac{f_n}{(\tan(\alpha/2)^2+1)^2(\tan(\beta/2)^2+1)^2}$$

where

$$\begin{aligned} f_n &= [[(t_a^2t_b^2+t_a^2+t_b^2+\lambda^2t_a^2t_b^2)\lambda^4-(2t_a^2t_b^2+2t_a^2+2t_b^2+1)](t_a+t_b+1) \\ &\quad +(2t_a^3t_b^3+2t_a^3t_b+t_a^3+t_a^2t_b+t_a^2+2t_at_b^3+t_at_b^2+2t_at_b+t_a+t_b^3 \\ &\quad +t_b^2+t_b+1)\lambda^2](t_a+t_b+1)\lambda^2 \\ t_a &= \tan(\alpha/2) \\ t_b &= \tan(\beta/2) \end{aligned}$$

The quantifier elimination[2] program QEPCAD [9] has proved that the logical formula

$$\forall t_a\, \forall t_b \quad f_n \le 0$$

is equivalent to the formula $\lambda = 0$. This shows that for the special case $\tau = \mu = \lambda \neq 0$ and $\gamma = \pi/2$ the absolute value of the amplification factor is greater than one and so the scheme is unstable. So the scheme is unstable for $\tau = \mu = \lambda \neq 0$ and most probably unconditionally unstable. Numerical sampling has shown that it is unstable for all non-zero values of λ, μ, τ.

The predictor scheme (4.3) is stable as it is a positive scheme if $\max(|\lambda|, |\mu|, |\tau|) \le 1$, so also the two step Lax-Friedrichs scheme is stable.

The composite schemes CFLFn are constructed as in 2D (3.8) and consist of $n-1$ CF steps and one LF step. For composite schemes the amplification factor is too complicated to be analyzed algebraically. We have analyzed the stability by numerical sampling and we have found that for small n the stability region of the composite scheme is quite a large subset of the cube $|\lambda| \le 1, |\mu| \le 1, |\tau| \le 1$, see the Fig. 4.2 for the stability region of CFLF2 for positive λ, μ, τ (the stability region is between the plotted surface and the plane $\tau = 0$ for $0 \le \lambda \le 1, 0 \le \mu \le 1$).

For several small n we have search the maximal r_n so that the CFLFn scheme is stable for all $|\lambda| < r_n, |\mu| < r_n, |\tau| < r_n$. r_n has been calculated by numerical sampling and its values are given in the Table 4.1.

To get a better insight into the stability properties of the composite schemes we have also considered the dependence of the effective amplification factor $|f|^{1/n}$ (i.e. the amplification factor per one time step) on the angles α, β, γ. In Fig. 4.3 we present this dependence for the case $\alpha = \beta = \gamma$ and $\lambda = \mu = \tau = 0.9$ for several composite CFLFn schemes. Note that the CFLF3 scheme slightly overshoots the value one so it is unstable for $\lambda = \mu = \tau = 0.9$ as we have already seen from the Table 4.1.

[2] Quantifier elimination (QE) is the procedure which transforms the formula

$$Q_1x_1 \in R,\ Q_2x_2 \in R, \cdots, Q_kx_k \in R, \quad F(x_1, \cdots, x_m),$$

where $m \ge k$, $Q_i, i = 1, \cdots, k$ are quantifiers $\forall$ (for all) or $\exists$ (there exists) and F is an arbitrary logical combination of polynomial equations or inequalities in the real variables $x_1, \cdots, x_m$, into the equivalent formula which does not contain any quantifier and contains only non-quantified variables $x_{k+1}, \cdots, x_m$ and is again a logical combination of polynomial equations and inequalities. In [20] Tarski has proved that QE is possible and in [21] he gave the algorithm for doing QE, however, the complexity of the algorithm was prohibitive as it cannot be bound by any finite tower of exponential functions. In [3] Collins presented a new method for QE by the cylindrical algebraic decomposition (CAD) with double exponential complexity. Based on this Hong [9] in cooperation with others developed the program QEPCAD (Quantifier Elimination by Partial Cylindrical Algebraic Decomposition) which incorporates many important improvements of the original CAD algorithm and which is the best QE program implemented up to now.

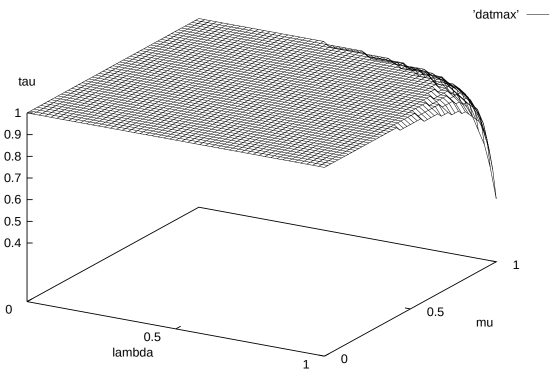

FIG. 4.2. *Stability region (between the plotted surface and the plane $\tau = 0$ for $0 \leq \lambda \leq 1, 0 \leq \mu \leq 1$) of the 3D CFLF2 composite scheme.*

TABLE 4.1
Maximal values of r_n so that the whole cube $(-r_n, r_n)^3$ is inside the stability region of the CFLFn scheme in λ, μ, τ space.

n	r_n
2	0.9299
3	0.8979
4	0.8770
5	0.8602

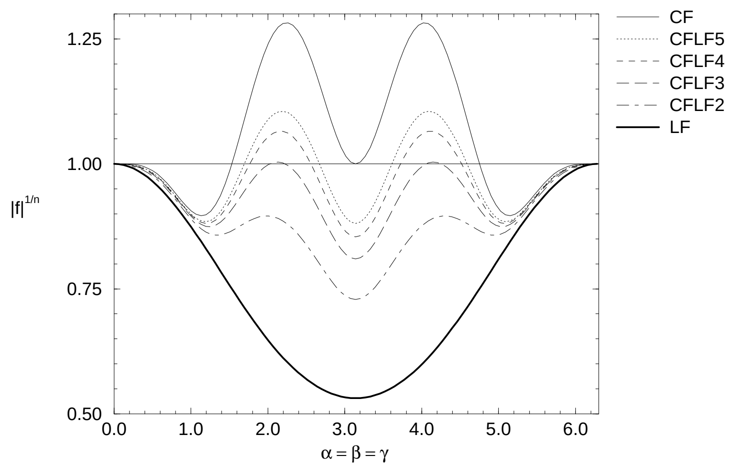

FIG. 4.3. *Dependence of the effective amplification factor per one time step on angles $\alpha = \beta = \gamma$ for the case $\lambda = \mu = \tau = 0.9$ for CF,CFLF5,CFLF4,CFLF3,CFLF2,LF schemes (in the order from top to down in the figure as in the legend).*

5. A second order composite. It would be desirable to have a composite which was as efficient as as LWLF or CFLF and which had at least as good resolving power but which was second order accurate for smooth flows. We have taken a preliminary step in this direction by using a second order diffusive WENO type scheme to replace the Lax-Friedrichs step. We thank Guang-Shan Jiang for graciously giving us the WENO code and for assisting in its implementation. We have modified this code to eliminate the eigenvector decomposition and we just use the WENO procedure on the conserved variables, an idea which is *not* recommended by the author of the code. Details of the full WENO method are in [11].

For the system

$$U_t = f_x(U)$$

WENO is a method of lines, solving the system of ordinary differential equations

$$U_t = \frac{1}{\Delta x}(F_{i+1/2} - F_{i-1/2}) = R_i$$

by a Runge-Kutta method, in our case it is just Heun's method. The numerical fluxes are obtained as follows. First, let

$$\begin{aligned} df^+_{i+1/2} &= \frac{1}{2}[f_{i+1} - f_i + \alpha(U_{i+1} - U_i)] \\ df^-_{i+1/2} &= \frac{1}{2}[f_{i+1} - f_i - \alpha(U_{i+1} - U_i)], \end{aligned}$$

and

$$\begin{aligned} C^-_i &= s^-_i(df^-_{i+1/2} - df^-_{i-1/2}) \\ C^+_{i+1} &= s^+_{i+1}(df^+_{i+3/2} - df^+_{i+1/2}), \end{aligned}$$

where the $s^\pm$ are certain diagonal weight matrices defined below. Then

$$F_{i+1/2} = \frac{1}{2}(f_{i+1} + f_i) - (C^+_{i+1} + C^-_i).$$

The weights are, for each component, given by

$$\begin{aligned} t_1 &= [10^{-6} + (df^-_{i-1/2})^2]^2 \\ t_2 &= [10^{-6} + (df^-_{i+1/2})^2]^2 \\ s^-_i &= \frac{t_2}{2(2t_1 + t_2)}, \end{aligned}$$

and

$$\begin{aligned} t_1 &= [10^{-6} + (df^+_{i+3/2})^2]^2 \\ t_2 &= [10^{-6} + (df^+_{i+1/2})^2]^2 \\ s^+_{i+1} &= \frac{t_2}{2(2t_1 + t_2)}. \end{aligned}$$

For a two-dimensional problem each dimension is treated in this way.

For the time advance the procedure is

$$\hat{U} = U^n + \Delta t R(U^n)$$
$$U^{n+1} = \frac{1}{2}\left(U^n + \hat{U} + \Delta t R(\hat{U})\right)$$

We choose α to be twice the maximum of $|u \pm c|$ taken over the grid, and instead of (3.9) we use

$$\max(|u \pm c|\Delta t/\Delta x + |v \pm c|\Delta t/\Delta y) \leq 1/4 \tag{5.1}$$

This choice is dictated by non-optimal stability of WENO and by some numerical experimentation. The one dimensional problem below was not sensitive to these values, but this choice worked best for Noh's problem.

The composites are LWCWn in one dimension, CFCWn in two, where CW stands for component-wise WENO.

For the first shallow water problem we compare CW with 250 points with the exact solution got by LWLF4 with 2000 points, see Fig. 5.1. CW is considerably better than LF (see Fig. 2.1) as it resolves shocks and their heights quite well.

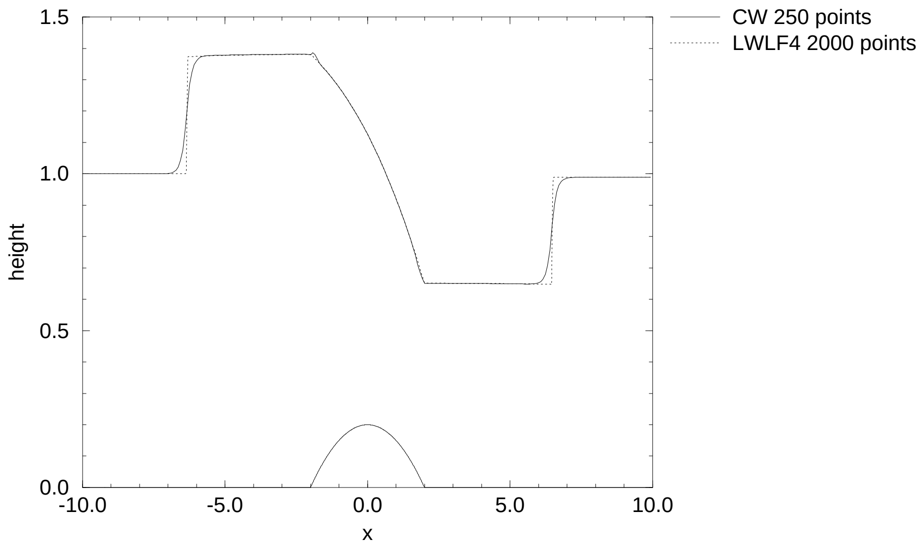

FIG. 5.1. *Comparison of heights for the shallow water problem with $b_c = 0.2, u_0 = 1$ at $t = 20$ calculated by component-wise WENO on 250 points and exact solution by LWLF4 on 2000 points.*

Next we compare the composites LWLF4 and LWCW4 for the same case with 250 points, see Fig. 5.2. Composition works again quite well. LWCW4 gives steeper shocks and resolves slightly better the heights of the shocks than LWLF4, however it has overshoots on the shock. A small overshoot appears also when LWCW4 is computed on the fine grid with 2000 points.

We have repeated with the CFCW4 scheme the computation of 2D Riemann problems for ideal gas dynamics done in §3.1 with the CFLF4 scheme. The results as contour plots are presented in Fig. 6.1 for the configuration 4 and in Fig. 6.2 for the

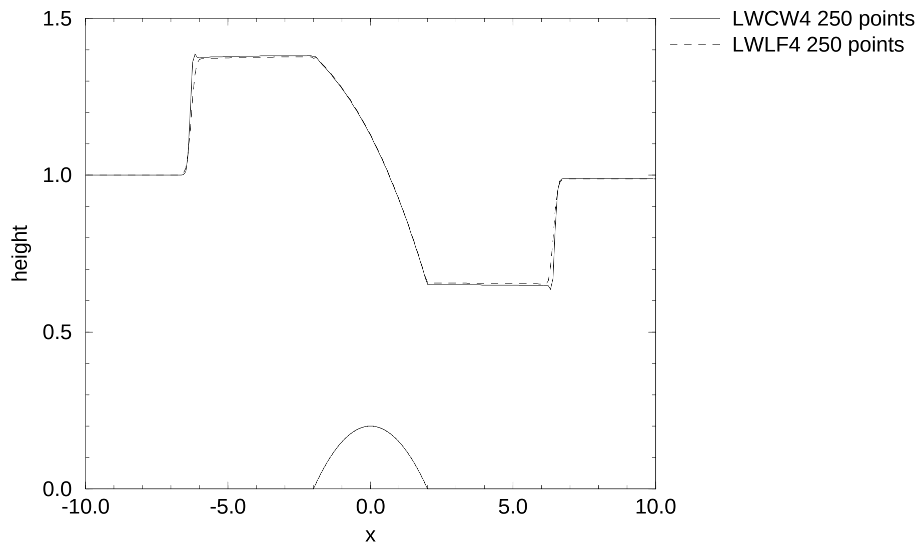

FIG. 5.2. *Comparison of heights for the shallow water problem with* $b_c = 0.2, u_0 = 1$ *at* $t = 20$ *calculated by LWCW4 and LWLF4 on 250 points.*

configuration 6. We have used again 400 by 400 grid and CFL limit 1 for CF steps and 1/4 for CW steps. The CFCW4 results are noisier than CFLF4 results and they have also overshoot on the curved shock for the configuration 4.

For Noh's problem the results of the CFCW4 scheme are as good or even slightly better than the results obtained in §3.1 by the CFLF4 scheme. The symmetry of the solution is again nice as shown on the surface plot in Fig. 3.5 for CFLF4 scheme. The comparison of CFCW4 and CFLF4 schemes is shown in Fig. 3.6 which shows the variation of the density along the diagonal $x = y$. As seen in this figure the CFCW4 scheme resolves slightly better the value 16 of the density behind the shock. The computation has been done again on the 75 by 75 grid.

6. Comments. We have proposed and tested some new descendents of the Lax-Friedrichs difference scheme obtained by globally composing a second order accurate oscillatory scheme with either a first order or second order diffusive scheme. The oscillatory passes seem to contain sufficient solution information which is revealed by the filtering diffusive passes. The resulting schemes are robust and show excellent resolution of both discontinuous and smooth solutions of hyperbolic systems in one and two dimensions, although the second order composite was noisier for the two-dimensional Riemann problem. We have found that three oscillatory steps followed by one diffusive step seems optimal in most cases. We showed the optimal stability of a variant of Lax-Friedrichs and a new second-order accurate scheme for constant coefficient scalar advection. For the gas dynamic equations our numerical results using (3.9) as the stability condition indicate that these schemes remain optimally stable, but a theoretical justification of this is lacking. Note that the Lax-Friedrichs variant surely has positive matrix coefficients in the linear case if Δt is small enough and is therefore L_2-stable by a theorem of Friedrichs ([16]), but for Δt only restricted by the CFL condition in each dimension, each coefficient is a symmetric product of positive matrices which is not necessarily positive. We have not tried to make a serious comparison of computational efficiency for these methods, but because they consist of very simple difference schemes not using an eigenvector decomposition or a precise Riemann solver they are quite fast. For example, the predictor- corrector and component-wise WENO (CWENO) composite was about 10 times faster then CWENO alone (not shown) on configuration 4 because of (5.1). In three dimensions a natural extension of the predictor-corrector scheme is unstable, but the composite with the first order diffusive step is sub-optimally stable.

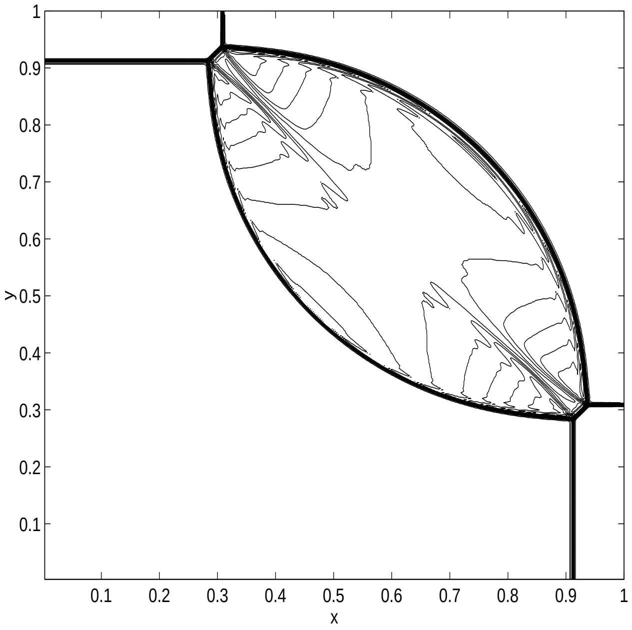

FIG. 6.1. *Contour plot of density for the 2D Riemann problem for an ideal gas for configuration 4 done with the CFCW4 scheme at* $t = 0.25$*, 356 time steps,* $\Delta x = \Delta y = 1/400$

Acknowledgements. Both authors were partially supported by the CHAMMP program of the US Department of Energy.

R. Liska would like to thank the Institute for Geophysics and Planetary Physics of the Los Alamos National Laboratory for hosting his visit at Los Alamos.

We would like to thank Misha Shashkov for suggesting Noh's problem as a test. We also want to thank Guang-Shan Jiang for sharing his elegant WENO code with us and for patiently answering our questions about the method. We are grateful to Clothilde Bon and Alain-Yves LeRoux for pointing out an error in an earlier version.

REFERENCES

[1] D. Book, J. Boris, and K. Hain, *Flux corrected transport II: Generalizations of the method*, J. Comp. Phys, 18 (1975), pp. 248–283.

[2] T. Boukadida and A.-Y. LeRoux, *A new version of the two-dimensional Lax-Friedrichs scheme*, Math. Comp., 63 (1994), pp. 541–553.

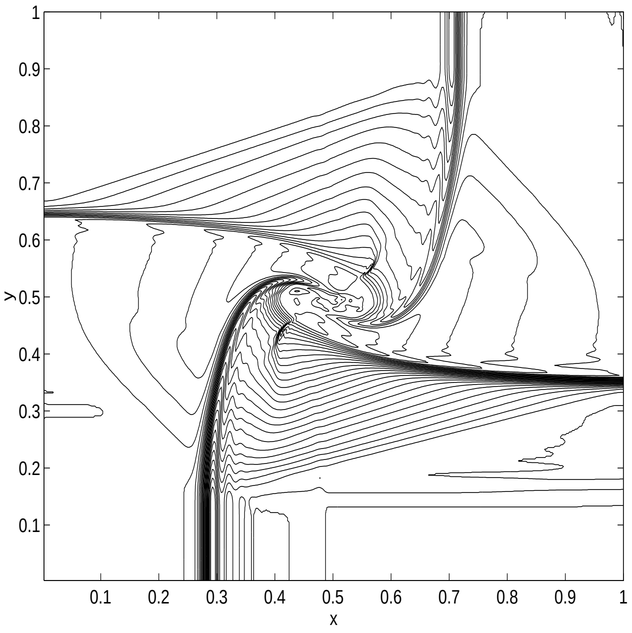

FIG. 6.2. *Contour plot of density for the 2D Riemann problem for an ideal gas for configuration 6 done with the CFCW4 scheme at* $t = 0.25$*, 386 time steps,* $\Delta x = \Delta y = 1/400$

[3] G. E. COLLINS, *Quantifier elimination in the elementary theory of real closed fields by cylindrical algebraic decomposition*, in Lecture Notes in Computer Science, Berlin, 1975, Springer-Verlag, pp. 134–183. Vol. 33.

[4] B. EILON, D. GOTTLIEB, AND G. ZWAS, *Numerical stabilizers and computing time for second order accurate schemes*, J. Comp. Phys., 9 (1972), pp. 387–397.

[5] B. EINFELDT, *On godunov-type methods for gas dynamics*, SIAM J. Numer Anal., 25 (1988), pp. 294–318.

[6] B. ENGQUIST, P. LÖTSTEDT, AND B. SJÖGREEN, *Nonlinear filters for efficient shock computation*, Math. Comp., 186 (1989), pp. 509–537.

[7] A. HARTEN AND G. ZWAS, *Self-adjusting hybrid schemes for shock computations*, J. Comp. Phys., 6 (1972), pp. 568–583.

[8] A. C. HEARN, *REDUCE user's manual, version 3.6*, Tech. Rep. RAND Publication CP 78 (Rev. 7/95), RAND, Santa Monica, 1995.

[9] H. HONG, *Improvements in CAD-based Quantifier Elimination*, PhD thesis, The Ohio State University, 1990.

[10] D. D. HOUGHTON AND A. KASAHARA, *Nonlinear shallow fluid flow over an isolated ridge*, Comm. Pure Appl. Math., 21 (1968), pp. 1–23.

[11] G.-S. JIANG AND C.-W. SHU, *Efficient implementation of weighted eno schemes*, J. Comp. Phys., 126 (1996), pp. 202–228.

[12] P. D. LAX AND X.-D. LIU, *Solution of two dimensional Riemann problem of gas dynamics by positive schemes*, SIAM J. on Scientific Comp., (1996). to appear.

[13] A.-Y. LEROUX AND P. QUESSEVEUR, *Convergence of an anti-diffusion lagrange-euler scheme for quasi-linear equations*, SIAM J. Numer. Anal., 63 (1984), pp. 985–994.

[14] R. LISKA AND L. DRSKA, *FIDE: A REDUCE package for automation of FInite difference method for solving pDE*, in ISSAC '90, Proceedings of the International Symposium on Symbolic and Algebraic Computation, Tokyo, August 20-24, 1990, S. Watanabe and M. Nagata, eds., New York, 1990, ACM Press, Addison Wesley, pp. 169–176.

[15] R. LISKA AND B. WENDROFF, *Analysis and computation with multi-layer fluid models*, Tech. Rep. LA-UR 96-384, Los Alamos National Laboratory, Los Alamos, 1996. submitted to J. Comp. Phys.

[16] X.-D. LIU AND P. D. LAX, *Positive schemes for solving multi-dimensional hyperbolic systems of conservation laws*, CFD Journal, 5 (1996), pp. 1–24.

[17] W. F. Noh, *Errors for calculations of strong shocks using an artificial viscosity and artificial heat flux*, J. Comp. Phys., 72 (1987), pp. 78–120.
[18] R. D. Richtmyer and K. W. Morton, *Difference Methods for Initial Value Problems*, John Wiley, New York, 1967. 2nd Ed.
[19] C. W. Schulz-Rinne, J. P. Collins, and H. M. Glaz, *Numerical solution of the Riemann problem for two-dimensional gas dynamics*, SIAM J. Sci. Comput., 14 (1993), pp. 1394–1414.
[20] A. Tarski, *The completness of elementary algebra and geometry*, 1930. Reprinted in 1967.
[21] ———, *A Decision Method for Elementary Algebra and Geometry*, Univ. of California Press, Berkeley, 1951. 2nd Ed.
[22] B. Wendroff, *Well-posed problems and stable difference operators*, SIAM J. Numer. Anal., 5 (1968), pp. 71–82.

Addendum. One of the referees raised several important points that have been addressed in the body of the paper. That referee also wondered about the accuracy of the composite schemes on a smooth problem. We have computed the periodic solution given by [11]

$$\rho(x,y,t) = 1 + 0.2\sin(\pi(x+y-t(u+v))), \quad u,v,p \text{ constants}$$

of the Euler equations for ideal gas. Here is a table showing the L_1 errors and ratios.

TABLE 6.1
L_1 errors and errors ratios for the smooth problem for LF, CFLF4, CFCW4, CF schemes. Ratios are ratios of the error with given Δx with the error with half space step, which is shown on the following line.

Δx	LF		CFLF4		CFCW4		CF	
	error	ratio	error	ratio	error	ratio	error	ratio
0.04	$1.5\ 10^{-2}$	2.00	$4.5\ 10^{-3}$	2.25	$3.4\ 10^{-4}$	3.92	$3.6\ 10^{-4}$	4.01
0.02	$7.6\ 10^{-3}$	1.97	$2.0\ 10^{-3}$	1.99	$8.7\ 10^{-5}$	4.00	$9.1\ 10^{-5}$	4.00
0.01	$3.8\ 10^{-3}$	1.98	$1.0\ 10^{-3}$	2.05	$2.1\ 10^{-5}$	3.95	$2.3\ 10^{-5}$	4.00
0.005	$1.9\ 10^{-3}$		$4.9\ 10^{-4}$		$5.5\ 10^{-6}$		$5.7\ 10^{-6}$	

The table shows that CFLF4 is first order, but more accurate than LF, while CFCW4 is second order having for this smooth problem the same accuracy as CF alone.